



**HAL**  
open science

## **Binding of pulmonary surfactant proteins to carbon nanotubes; potential for damage to lung immune defense mechanisms**

Carolina Salvador-Morales, Paul Townsend, Emmanuel Flahaut, Catherine Vénien-Bryan, Alexis Vlandas, Malcolm L. H. Green, Robert B. Sim

### ► **To cite this version:**

Carolina Salvador-Morales, Paul Townsend, Emmanuel Flahaut, Catherine Vénien-Bryan, Alexis Vlandas, et al.. Binding of pulmonary surfactant proteins to carbon nanotubes; potential for damage to lung immune defense mechanisms. *Carbon*, 2007, vol. 45, pp. 607-617. 10.1016/j.carbon.2006.10.011 . hal-00808254

**HAL Id: hal-00808254**

**<https://hal.science/hal-00808254>**

Submitted on 5 Apr 2013

**HAL** is a multi-disciplinary open access archive for the deposit and dissemination of scientific research documents, whether they are published or not. The documents may come from teaching and research institutions in France or abroad, or from public or private research centers.

L'archive ouverte pluridisciplinaire **HAL**, est destinée au dépôt et à la diffusion de documents scientifiques de niveau recherche, publiés ou non, émanant des établissements d'enseignement et de recherche français ou étrangers, des laboratoires publics ou privés.



## Open Archive Toulouse Archive Ouverte (OATAO)

OATAO is an open access repository that collects the work of Toulouse researchers and makes it freely available over the web where possible.

This is an author-deposited version published in: <http://oatao.univ-toulouse.fr/>  
Eprints ID : 2466

**To link to this article :**

URL : <http://dx.doi.org/10.1016/j.carbon.2006.10.011>

**To cite this version :** Salvador-Morales, Carolina and Townsend, Paul and Flahaut, Emmanuel and Vénien-Bryan, Catherine and Vlandas, Alexis and Green, Malcolm L. H. and Sim, Robert B. ( 2007) [\*Binding of pulmonary surfactant proteins to carbon nanotubes; potential for damage to lung immune defense mechanisms.\*](#) Carbon, vol. 45 (n° 3). pp. 607-617. ISSN 0008-6223

Any correspondence concerning this service should be sent to the repository administrator: [staff-oatao@inp-toulouse.fr](mailto:staff-oatao@inp-toulouse.fr)

# Binding of pulmonary surfactant proteins to carbon nanotubes; potential for damage to lung immune defense mechanisms

Carolina Salvador-Morales<sup>a,b</sup>, Paul Townsend<sup>b</sup>, Emmanuel Flahaut<sup>c</sup>, Catherine Vénien-Bryan<sup>d</sup>, Alexis Vlandas<sup>e</sup>, Malcolm L.H. Green<sup>a</sup>, Robert B. Sim<sup>b,\*</sup>

<sup>a</sup> *Inorganic Chemistry Laboratory, University of Oxford, South Parks Road, Oxford OX1 3QR, United Kingdom*

<sup>b</sup> *MRC Immunochemistry Unit, Department of Biochemistry, University of Oxford, South Parks Road, Oxford OX1 3QU, United Kingdom*

<sup>c</sup> *Centre Interuniversitaire de Recherche et d'Ingénierie des Matériaux, Université Paul Sabatier, 118 Route de Narbonne, Toulouse 31062, France*

<sup>d</sup> *Laboratory of Molecular Biophysics, Department of Biochemistry, University of Oxford, South Parks Road, Oxford, OX1 3QU, United Kingdom*

<sup>e</sup> *Department of Materials, University of Oxford, Parks Road, Oxford OX1 3PH, United Kingdom*

## Abstract

Potential pulmonary toxicity of carbon nanotubes is a research area that has received considerable attention. Surfactant proteins A and D (SP-A and SP-D) are collectin proteins that are secreted by airway epithelial cells in the lung. They play an important role in first-line defense against infection within the lung. The aim of this study was to investigate the interaction between carbon nanotubes and proteins contained in lung surfactant. By using sodium dodecyl sulphate-polyacrylamide gel electrophoresis (SDS-PAGE), Western Blotting, a novel technique of affinity chromatography based on carbon nanotube–Sepharose matrix [1] and electron microscopy data it was shown that SP-A and SP-D selectively bind to carbon nanotubes. The binding was Ca<sup>2+</sup>-ion dependent, and was variable between batches of nanotubes. It was therefore likely to be mediated by surface impurities or chemical modifications of the nanotubes. Chronic level exposure to carbon nanotubes may result in sequestration of SP-D and SP-A. Absence of these proteins in knockout mice leads to susceptibility to lung infection and emphysema.

## 1. Introduction

Carbon nanotubes are widely considered to be one of the most versatile families of new materials and will be instrumental in driving forward the nanotechnology industrial revolution in the coming decade. Reported uses in fields as diverse as polymers, electronics or even health care, while promising significant improvements in quality of life, will require production of nanotubes to reach industrial levels. It is therefore essential to investigate thor-

oughly the effects that carbon nanotubes might have on human health. Three distinct entry routes into the human body are recognised: ingestion, penetration through the skin and inhalation. The last probably constitutes the highest risk as it is notably difficult to deal reliably with suspension in air of extremely small particles. Carbon nanotubes tend to form aggregates, many of which will not penetrate to the lung alveoli when inhaled. However, non-aggregated carbon nanotubes may, because of their small size, penetrate to the alveoli of the lungs, where they may interact with surfactant proteins and lipids.

While *in vivo* toxicity studies previously reported represent an important first step in highlighting the possible risks associated with exposure to carbon nanotubes, the protocols they rely upon may have produced artefacts

\* Corresponding author. Fax: +44 1865 275729.  
E-mail address: bob.sim@bioch.ox.ac.uk (R.B. Sim).

that can be difficult to distinguish from effects produced by nanotubes themselves. For example, in instillation studies the aggregation of nanotubes produces mortality by airway obstruction in rats as reported by Warheit et al. [2] and Muller et al. [3]. Further studies are needed to elucidate how carbon nanotubes interact with host pulmonary systems at the molecular level.

The lungs are an important interface between the host and an environment that contains a plethora of potentially harmful microorganisms. The immune defense of the lung involves the pulmonary surfactant, a complex mixture of lipids, phospholipids, and proteins important for normal respiratory function [4]. Two of these surfactant proteins are SP-A and SP-D (Fig. 1), which belong to a family known as the collectins, as they contain a collagenous region and a C-type lectin domain. A major biological role of the collectins is to bind to targets (e.g., microorganisms and allergens) by recognizing patterns of carbohydrate distribution at their surface and to enhance phagocytosis/clearance of the targets. Thus, they play an important role in first-line immune defenses within the lung.

In this communication we report for the first time the selective binding of SP-A and SP-D to carbon nanotubes. These results enable us to shed new light on previously published toxicity studies and also reveal hitherto uncharacterised variability in the nanotubes. The results suggest that long-term exposure to inhalation of nanotubes has

the potential to enhance susceptibility to infection and emphysema.

## 2. Materials and methods

### 2.1. Synthesis of carbon nanotube samples

Catalytic vapor deposition double-walled nanotubes (DWNT) were made as described by Flahaut et al. [5]. After the synthesis the sample was washed with a concentrated aqueous solution of HCl (ca. 12.1 M) to dissolve all the accessible catalyst (including all MgO-based catalyst and non-protected metal particles). The sample was filtered and washed to neutrality. A final rinse was given with ethanol before drying. Subsequently, the carbon nanotube sample was dried at 80 °C in air.

### 2.2. Characterisation of carbon nanotubes

#### 2.2.1. Elemental analysis

Plasma atomic emission spectroscopy studies were performed on “as-made” DWNTs to quantify the remaining traces of metal element impurities after their synthesis, and the carbon content. It was found that DWNTs contained 1.9% (w/w) Mo, 94% (w/w) carbon, 4% (w/w) Co and some traces of O<sub>2</sub> (see Table 1).

#### 2.2.2. Specific surface area

The surface area of DWNTs was measured with a Sorptomatic 1990 (ThermoQuest) instrument. This instrument is based on the static volumetric principles, using the multiple-point method and nitrogen as the adsorption gas. The sample was degassed at 300 °C for 1.50 h in a vacuum of  $\sim 10^{-3}$  torr before exposure to analysis conditions (see Table 1).

#### 2.2.3. Transmission electron microscopy

A very small amount of DWNTs was suspended in ethanol, sonicated for 5 min in a bath sonicator and dropped onto a copper TEM grid. Subsequently, the sample was analysed by JEOL 4000EX High Resolution Transmission Electron Microscopy (see Fig. 2).

#### 2.2.4. Infrared spectroscopy

Fourier-transform infrared (FTIR) spectroscopy data were collected using a Nicolet Magna 560 FTIR. The infrared spectra were taken as reported by Kim et al. [6]. Briefly, the nanotube material was first ultrasonicated in 2-propanol using a low power ultrasonic bath (Ultrawave 300). Several drops of the suspension were then deposited onto ZnSe substrates maintained in air at about 70 °C. The solvent from each drop was allowed to evaporate before the next drop was added. The sample was then heated for 4 h at 70 °C in order to completely evaporate the 2-propanol.

### 2.3. Protein interaction with carbon nanotubes

#### 2.3.1. Preparation of Bronchoalveolar Lavage Fluid (BALF)

Bronchoalveolar Lavage Fluid (BALF) was obtained from alveolar proteinosis patients (Royal Brompton Hospital, London, UK). These patients have a much higher concentration of lung surfactant protein than

Table 1  
Characteristics of individual DWNTs

	DWNTs
Length	(> 500 nm)
Average inner diameter (nm)	1.3 nm
Average outer diameter (nm)	3.11 nm
Specific surface area (m <sup>2</sup> /g)	1032. 14
Carbon content	94% (w/w)
Metallic impurities	1.9% (w/w) Mo, 4% (w/w) Co and some traces of O <sub>2</sub>

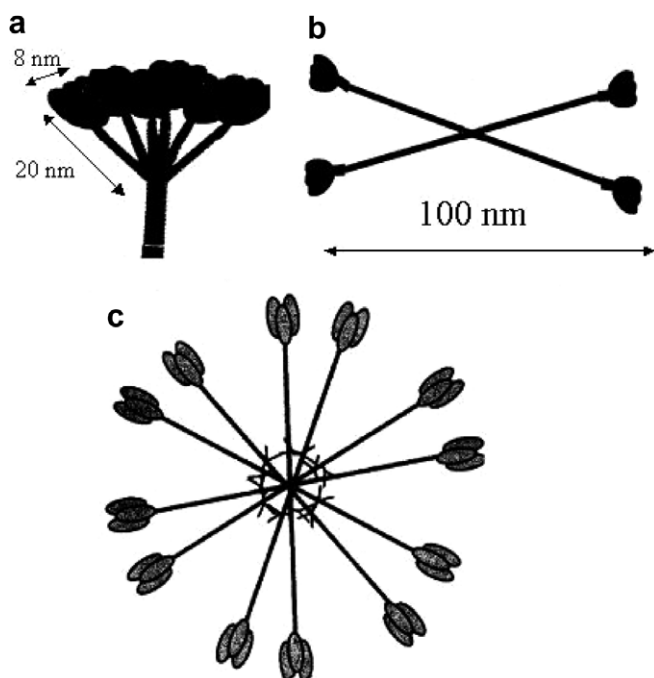


Fig. 1. Schematic representation of SP-A and SP-D. SP-A is predominantly assembled as octadecamers consisting of six trimeric subunits of arm length 20 nm (a). SP-D is predominantly assembled as dodecamers consisting of four homotrimeric subunits (b), with arm length of 46 nm, but multimers of dodecamers linked at the N-terminal have been observed (c). Picture taken from Murray, E. (2001), D.Phil thesis, University of Oxford [34].

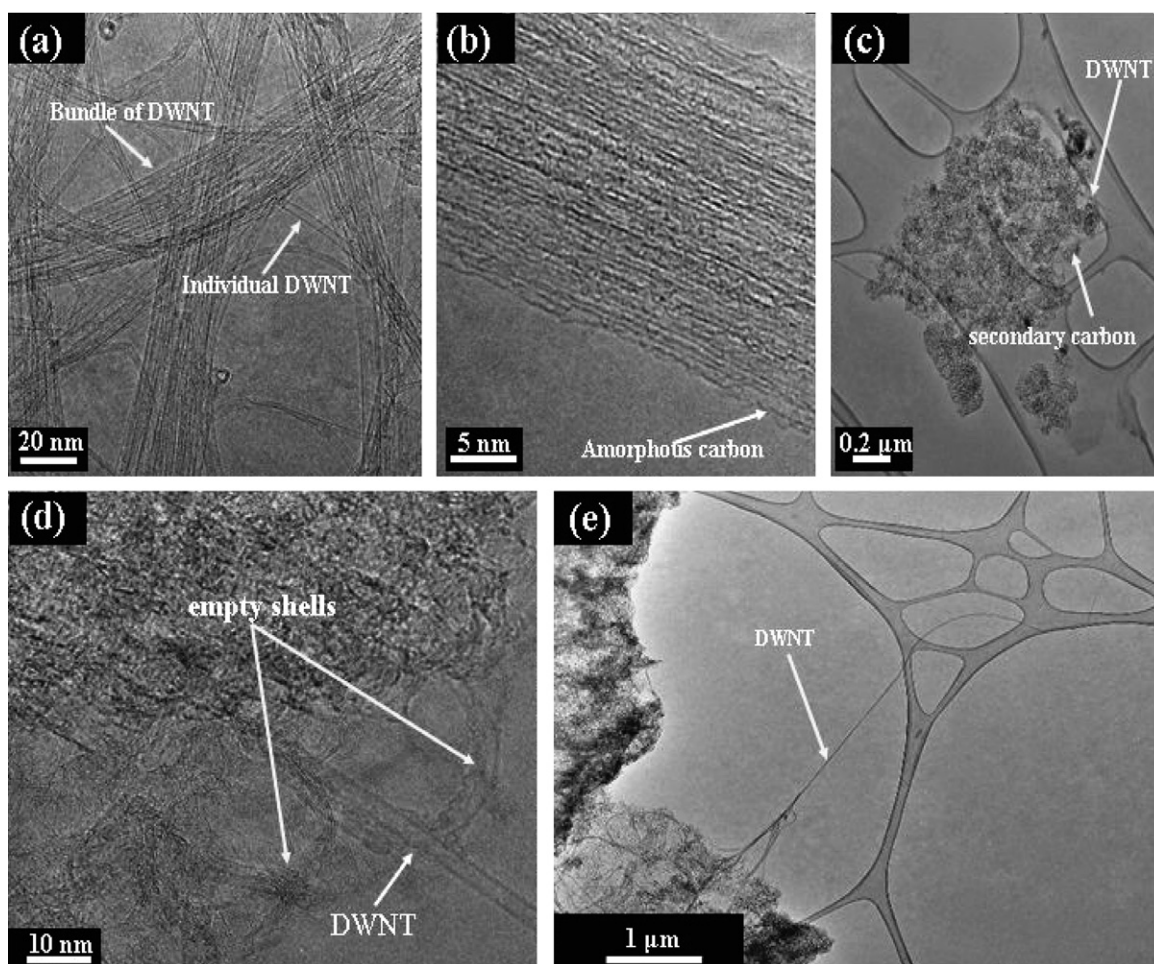


Fig. 2. *Quality analysis of DWNT by TEM studies.* (a) Image showing the overall morphology of DWNTs. Bundled and individual DWNTs are indicated by white arrows. (b) High magnification micrograph showing the good degree of crystallinity of the DWNTs. Note that some amorphous carbon is present on these DWNTs, as indicated by the arrows, although overall there is very little of it in the sample. (c) Low magnification image depicts secondary carbon forms found in the DWNT sample. “Secondary carbon forms” refer to graphitic shells (which held catalyst but the metal has been removed), amorphous carbon (byproduct of synthesis) and carbon-encapsulated metal nanoparticles which can not be completely removed from the samples. (d) Higher magnification of (c) showing the graphitic nature of the shell. (e) Low magnification image showing the length of DWNTs.

normal. BALF from these patients is used in this work because the concentration of protein in BALF from normal lung is too low for use in practical binding experiments. SP-A and SP-D isolated from alveolar proteinosis BALF are accepted as having the same properties as SP-A, SP-D from BALF from healthy lungs [7,8]. The lungs were washed with 20 L of Phosphate buffered saline (PBS (8.2 mM  $\text{Na}_2\text{HPO}_4$ , 1.5 mM  $\text{KH}_2\text{PO}_4$ , 139 mM NaCl, 3 mM KCl, pH 7.4)). Ten litres of BALF was centrifuged at 2740 g for 40 min at 4 °C. After centrifugation, the supernatant was recovered and frozen at -20 °C.

### 2.3.2. Estimation of the protein concentration of the BALF supernatant samples

Protein concentration of several BALF supernatant patient samples was measured by the Bradford Method [9] using a kit (Bio-Rad, Hemel Hempstead, UK). A bovine serum albumin (BSA) standard curve was made and used to calculate the unknown protein in the samples tested.

### 2.3.3. Affinity chromatography based on carbon nanotube–Sephacose matrix

Experiments using BALF supernatant were carried out to determine whether proteins in BALF bind selectively to carbon nanotubes. Two Sepharose 4B (Amersham Bioscience, Bucks, UK) columns were set up: a larger Sepharose column (10 ml) (not containing carbon nanotubes),

and a small Sepharose column (1 ml, containing 10 mg DWNT suspended among the Sepharose beads). These were equilibrated in the running buffer (10 mM HEPES, 140 mM NaCl, 0.15 mM  $\text{CaCl}_2$ , pH 7.0). BALF supernatant (50 ml) was dialysed in the running buffer and passed through the large column to remove proteins which bind to Sepharose, then through the small column to bind proteins which interact with the carbon nanotubes. After this, each column was thoroughly washed with the running buffer. From each column, the resin was resuspended to a 1:1 slurry in the running buffer. One hundred microlitres of each slurry was centrifuged at 13,000 rpm for 5 min. The supernatants were removed. Fifty microlitres of SDS-PAGE sample buffer was added to the resins. Samples were incubated at 95 °C for 5 min and loaded on an SDS-PAGE gradient gel as described in Section 2.3.4. Proteins bands on the SDS-PAGE gel were stained, then excised from the gel and prepared for protein identification by tryptic peptide fingerprinting by mass spectrometry and N-terminal sequence analysis as indicated in Sections 2.3.5 and 2.3.6, respectively.

### 2.3.4. SDS-PAGE

The samples that required electrophoretic analysis were incubated at 95 °C for 5 min in sample buffer (0.2 M Tris, 8 M urea, 2% SDS, 0.2M EDTA, 40 mM dithiothreitol (DTT), adjusted to pH 8.2 with HCl) and

loaded on a 4–12% Novex Bis-Tris sodium dodecyl sulphate-polyacrylamide gel electrophoresis (SDS-PAGE) gradient gel (Invitrogen, Paisley, UK), then separated by electrophoresis for 50 min at 150 V using MES buffer (Invitrogen) in a Novex X Cell II Mini-cell gel apparatus. Proteins bands were stained with Simply Blue Safe Stain (Invitrogen).

### 2.3.5. Mass-spectrometry analysis of proteins

In order to identify the BALF supernatant proteins attached to DWNTs, mass-spectrometry analysis was conducted as follows. SDS-PAGE gel bands were destained 3 times for 20 min in 100  $\mu$ l 50 mM  $\text{NH}_4\text{HCO}_3$  in 50% (v/v) acetonitrile. The supernatant was discarded and gel pieces were soaked in 100  $\mu$ l of 80% (v/v) acetonitrile for 20 min. The acetonitrile was removed and gel pieces dried under vacuum for 30 min using a centrifugal evaporator [Speed-vac, Savant, USA]. The proteins in the gel pieces were re-reduced by swelling them in 50  $\mu$ l 10 mM dithiothreitol (DTT) in 100 mM  $\text{NH}_4\text{HCO}_3$  and incubating (45 min, 56 °C). Gel pieces were chilled to room temperature and DTT solution removed by aspiration. Fifty  $\mu$ l of 55 mM iodoacetamide in 100 mM  $\text{NH}_4\text{HCO}_3$  was added and the gel pieces were incubated for 30 min at room temperature to alkylate free SH groups. Liquid was removed and gel pieces were washed with  $\text{NH}_4\text{HCO}_3$ /acetonitrile as previously. Gel pieces were completely dried under vacuum, re-hydrated in 50  $\mu$ l 20 ng/ $\mu$ l trypsin in 100 mM  $\text{NH}_4\text{HCO}_3$  (Sigma sequence grade) and left to incubate at 37 °C overnight. The supernatant was removed and stored in a 0.5 ml conical centrifuge tube. Fifty  $\mu$ l of acetonitrile: trifluoroacetic acid (TFA): water (50:1:49 v/v) was added to the gel pieces and the samples agitated for 20 min at room temperature. The supernatant was removed and pooled with supernatant from the previous step before being dried under vacuum as before. The sample was reconstituted in 10  $\mu$ l 0.1% (v/v) TFA or 5  $\mu$ l if from a faint gel band. One  $\mu$ l of sample was mixed with 1  $\mu$ l of saturated  $\alpha$ -cyano matrix solution of which 0.5  $\mu$ l was loaded onto an Ettan MALDI-ToF Pro mass spectrometer (Amersham Biosciences) target slide for PMF (peptide mass fingerprint) analysis in reflectron mode. Proteins were identified by comparison of the spectra to a computer-generated database of tryptic peptides from known proteins using ProFound, the instrument's built-in search engine (Proteometrics LLC) which utilises the NCBI nr protein database (National Center for Biotechnology Information, Bethesda, USA).

### 2.3.6. N-terminal sequence analysis

Proteins which were not identified by mass spectrometry were subjected to N-terminal sequence analysis. Samples were reduced and run on SDS-PAGE (as in Section 2.3.4). The gel was electroblotted on to Novex 0.2  $\mu$ m PVDF membrane (Invitrogen) in a Novex blot module. The membrane was then stained with Coomassie Brilliant Blue. The bands of interest were excised from the PVDF membrane and washed extensively with 10% methanol in water prior to sequencing. Samples were then sequenced on an Applied Biosystems 494A "ProCise" protein sequencer (Applied Biosystems) using standard sequencing cycles.

### 2.3.7. Western blotting to detect SP-D

Protein transfer from SDS-PAGE gels to an Immobilon-P transfer membrane was carried out using a Biometra Fastblot B43 semi-dry transfer system. The gel and the membrane were soaked in transfer buffer (25 mM Tris, 232 mM glycine, 20% methanol) before application of a constant current at 50 mA for 70 min. The membrane was then blocked in PBS containing 5% (w/v) non-fat dried milk, 0.2% Tween-20, 0.5 mM EDTA (blocking buffer) overnight at 4 °C. The membrane was incubated with polyclonal biotinylated rabbit anti-human SP-D (4.2 mg/ml stock) (MRC Immunochemistry Unit, Oxford, UK) diluted 1:4000 in blocking buffer for 1 h at room temperature with shaking. After three washes with PBS containing 0.1% Tween-20 (wash buffer) the membrane was incubated with 10 ml of PBS – 0.1% Tween-20 – 2% BSA containing 1.5  $\mu$ l of streptavidin-peroxidase (Sigma) (S5512) for 30 min at room temperature. The membrane was washed three times as before and the proteins detected by the ECL Plus Western blotting detection system (Amersham Biosciences).

### 2.3.8. ELISA assay for SP-D

Purified IgG from polyclonal rabbit anti-human SP-D (161 ng per well) (MRC Immunochemistry Unit, Oxford, UK) in 0.1 M sodium carbonate buffer (pH 9.6) was coated on a Maxisorb 96-well plate (Nunc) for 16 h at 4 °C. The plate was washed three times in PBS – 0.05% Tween (PBST) and then blocked in the same buffer plus 3% (w/v) BSA for 1 h at 37 °C. Between each subsequent step the plate was washed in PBS – 0.05% Tween-20. BALF was diluted (2-fold serial dilutions) in PBS and 100  $\mu$ l added to each well followed by incubation at 37 °C for 4 h. This was done in duplicate. Following washing steps, an aliquot (100  $\mu$ l) of polyclonal biotinylated rabbit anti-human SP-D (1:1000 dilution of 4.2 mg/ml stock) (MRC Immunochemistry Unit, Oxford, UK) in PBST was added to each well and incubated for 2 h at 37 °C. After washing, 100  $\mu$ l of streptavidin peroxidase conjugate (Sigma) diluted 1:10,000 in blocking buffer was added for 30 min at 37 °C. The plate was developed with TMB peroxidase substrate (EIA substrate Kit, solution A) (BioRad) and the reaction was stopped with 100  $\mu$ l 2 M  $\text{H}_2\text{SO}_4$  and subsequently read at 450 nm (Titertek Multiskan Plus MKII). The standard was purified native SP-D serially diluted from 500 ng/ml to 0.98 ng/ml.

### 2.3.9. Quantification of BALF supernatant SP-D and SP-A bound to DWNT

Fifty ml of undiluted BALF supernatant previously dialysed in 10 mM HEPES, 140 mM NaCl, 0.15 mM  $\text{CaCl}_2$ , pH 7.0 was loaded onto a 1 ml Sepharose column containing 10 mg DWNT. After removing unbound proteins by exhaustive washes with the same buffer several aliquots of the DWNT–Sepharose mixture (5  $\mu$ l, 10  $\mu$ l) and BALF supernatant (5  $\mu$ l, 10  $\mu$ l) were analysed for bound SP-D protein by Western Blot. The resulting protein band was measured by a densitometer (Bio imaging system) (Synoptics, Cambridge, UK) and analysed by Gene tools software (Synoptics). SP-D concentration in the BALF was measured by ELISA – 109.62 ng/ml. For SP-A estimation several aliquots of the DWNT–Sepharose mixture (2.5  $\mu$ l, 5  $\mu$ l and 10  $\mu$ l), native SP-A (0.25, 0.5 and 1  $\mu$ g) and BALF supernatant (2.5  $\mu$ l, 5  $\mu$ l and 10  $\mu$ l) were loaded into SDS PAGE and stained by Coomassie Blue. The resulting protein bands were measured by a densitometer (as above) and analysed by Gene Tools Software.

### 2.3.10. Purification of SP-A and SP-D standards

SP-A and SP-D were purified from BALF as described in Refs. [10,11] respectively. The SP-A was kindly supplied by Roona Deb (MRC Immunochemistry Unit).

### 2.3.11. Transmission electron microscopy studies on the interaction between carbon nanotubes and surfactant proteins A and D

A small amount of DWNTs (approximately 400  $\mu$ g) was suspended in 10 mM HEPES, 140 mM NaCl, 0.15  $\text{CaCl}_2$ , pH 7.0 followed by incubation with SP-A or SP-D (50  $\mu$ g/ml final concentration in the sample buffer). The mixtures were incubated overnight at 4 °C. After incubation, samples were washed several times with 10 mM HEPES, 140 mM NaCl, 0.15  $\text{CaCl}_2$  mM, pH 7.0 to remove unbound materials. 2.5  $\mu$ l of this preparation was placed on a carbon film previously treated by glow discharge in air. After a few seconds of absorption, the grid was negatively stained with 2% uranyl acetate solution in water. The carbon grid was blotted and examined in the microscope. The images were recorded at a magnification of 60,000 times with a Philips CM120 transmission electron microscope operating at 100 kV (Laboratory of Molecular Biophysics, Biochemistry Department, Oxford University).

## 3. Results

SDS-PAGE analysis of DWNTs after exposure to BALF (Fig. 3, track 3) shows that in the presence of ethylene diamine tetra acetic acid (EDTA) almost no protein from the BALF supernatant binds to the DWNTs. However in the presence of  $\text{Ca}^{2+}$  ions several proteins

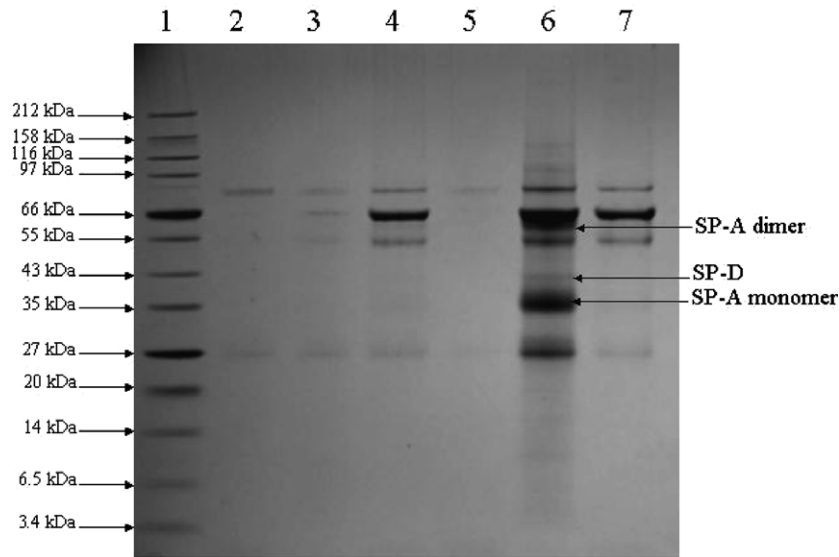


Fig. 3. *BALF supernatant proteins bound to DWNT in the presence of EDTA or CaCl<sub>2</sub>*. Fifty ml of undiluted BALF supernatant previously dialysed in 10 mM HEPES, 140 mM NaCl, 0.15 mM CaCl<sub>2</sub> was passed through a Sepharose column linked to a Sepharose–DWNT column as described in Section 2.3.3. After extensive washing in the running buffer, samples of the affinity resins were analysed by SDS-PAGE (reduced). Lane 1. Molecular weight marker; lane 2, 5, Control experiment (BALF supernatant proteins bound to Sepharose in EDTA, Ca<sup>2+</sup> respectively); lane 3. BALF supernatant proteins bound to DWNTs in the presence of 10 mM HEPES, 140 mM NaCl and 2 mM EDTA; lane 4, 7, BALF supernatant (10 µl); lane 6. BALF supernatant proteins bound to DWNTs in the presence of 10 mM HEPES, 140 mM NaCl, 0.15 mM CaCl<sub>2</sub>. Black arrows indicate the presence of SP-D and SP-A at 43 kD and 35 kDa, respectively. SP-A is seen as a monomer 35 kD and ~66 kDa dimer. In Fig. 3, the SP-A dimer is compressed under the albumin band.

(6–8 bands on SDS-PAGE) bind, and are easily detectable (Fig. 3, track 6). By mass spectrometry analysis the BALF supernatant proteins attached to DWNTs were identified (Fig. 4). Transferrin, Human Serum Albumin (HSA), and IgG were detectable, and the lung protein SP-A was prominent among the bound proteins. SP-A was not identifiable by tryptic peptide fingerprinting but was identified by N-terminal sequencing. Whereas the SP-A was prominent among the proteins bound to carbon nanotubes, it was not visible in the BALF (Fig. 3, tracks 4 and 7). A faint band above SP-A in Fig. 4 is in the appropriate migration position for the lung protein SP-D, but its abundance was too low to enable its identification by mass spectrometry. Western Blotting (Fig. 5) was used to assign unambiguously this band to SP-D. In Fig. 4, it is clear that SP-A and SP-D are concentrated by the DWNTs. Some transferrin, albumin and IgG (immunoglobulin) also bind, but are less enriched than SP-A, SP-D. There was negligible protein binding to the control Sepharose in either EDTA or CaCl<sub>2</sub> (Fig. 3, tracks 2 and 5).

Transmission electron microscopy studies confirmed the binding of SP-A and SP-D to DWNTs (Fig. 6C and E, respectively). Protein is bright against a darker background (negative stain). Individual carbon nanotubes, SP-A, and SP-D molecules are shown in Fig. 6A, B and D, respectively. They served as controls for the interaction between carbon nanotubes with SP-A/SP-D. Individual DWNT (4 nm in diameter, 533 nm in length) were imaged at a magnification of 60,000×. Their outer walls are clearly observed in Fig. 6A. At least eight SP-A “heads” are visible in Fig. 6B. They look like white round dots and are indicated

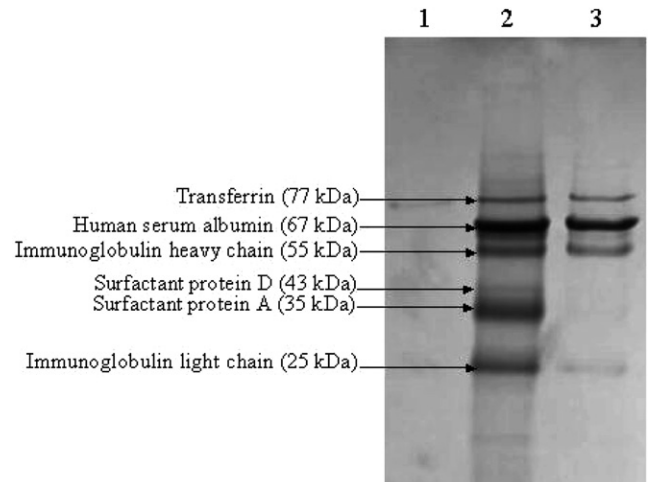


Fig. 4. *Selective binding of BALF supernatant proteins to DWNT*. Fifty ml of undiluted BALF supernatant previously dialysed in 10 mM HEPES, 140 mM NaCl, 0.15 mM CaCl<sub>2</sub> was passed through Sepharose and Sepharose–DWNT columns as described in Section 2.3.3. After extensive washing in the running buffer, samples of the affinity resins were analysed by SDS-PAGE (reduced). Lane 1. Control experiment (BALF supernatant proteins bound to Sepharose); lane 2. BALF supernatant proteins bound to DWNT–Sepharose, lane 3. BALF (10 µl). All the proteins indicated in the gels were identified by fingerprinting mass spectrometry except SP-A, which was detected by N-Terminal Sequence Analysis and SP-D that was identified by Western Blotting (see Section 2.3.7). In this picture SP-A dimer appears as a faint band below Human Serum Albumin.

by the black arrows. The collagen region is not seen in any SP-A molecule of this image probably due to its orientation on the grid, and the collagen region is too thin to be seen at



Fig. 5. BALF supernatant SP-D bound to DWNT and identified by Western blotting. Fifty ml of undiluted BAL fluid supernatant previously dialysed in 10 mM HEPES, 140 mM NaCl, 0.15 mM CaCl<sub>2</sub>, pH 7.0 was loaded onto Sepharose-DWNT as described in Section 2.3.3. After removing unbound proteins by exhaustive washes with the running buffer a suspension of the Sepharose-DWNT mixture was analysed for bound SP-D by Western Blotting. Lane 1. Sepharose-DWNTs (10 µl); lane 2. BALF supernatant (10 µl); lane 3: Native SP-D (0.5 µg).

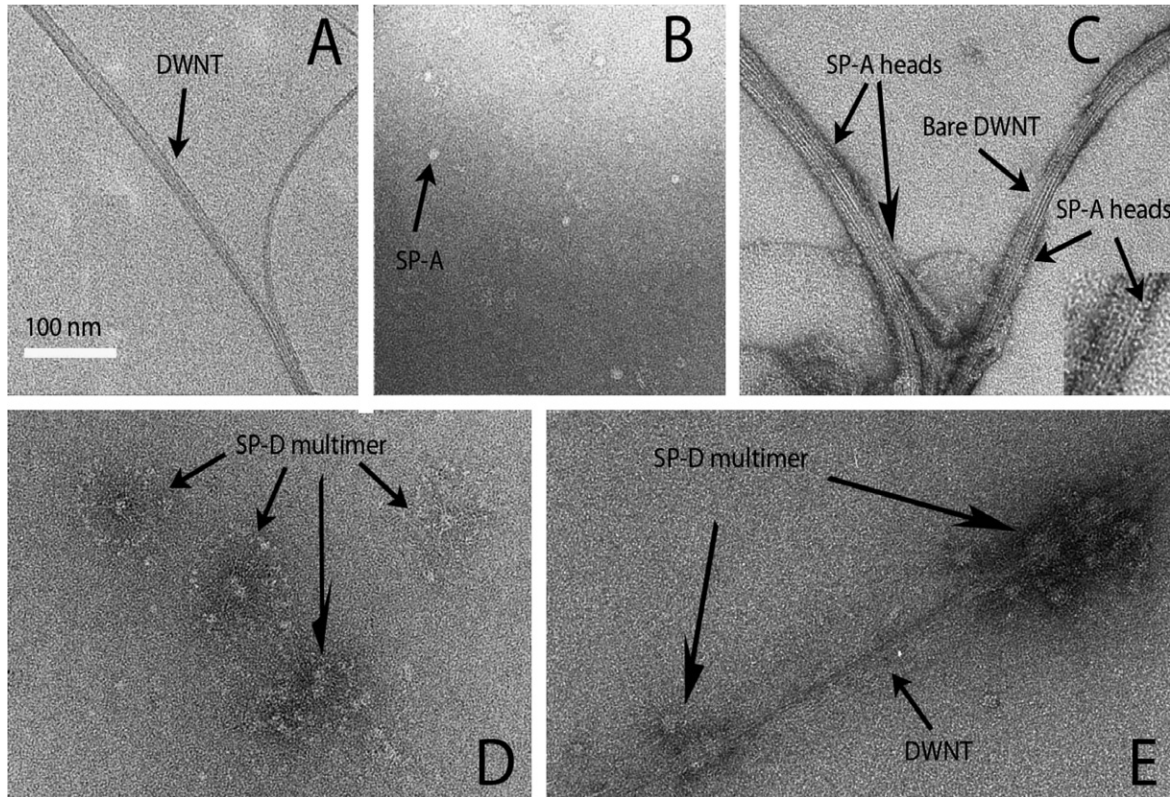


Fig. 6. Electron micrographs showing the binding of SP-A and SP-D to DWNT. (A) DWNTs, (B) SP-A alone, (C) SP-A attached to DWNTs. The inset in the right bottom corner of Fig. 6C shows a head of SP-A bound to DWNTs as pointed out by the black arrow. (D) SP-D alone, (E) SP-D attached to DWNTs.

this magnification. SP-A heads in this figure are approximately 8 nm diameter according to the scan bar (100 nm). This value is consistent with the one reported in literature [12] (see Fig. 1). Fig. 6C shows the decoration of DWNT bundles by SP-A heads. This phenomenon is easily observed at the external walls of the DWNTs. In this region, individual heads are located side by side (the heads are spaced regularly) making the distribution quite homogenous at the edge of DWNTs. The presence of the stain uranyl acetate, at the edge (black region) of the DWNTs allowed enhancement of the contrast and detection of SP-A. The dimensions of the SP-A heads in this figure are consistent with the dimension of SP-A heads presented in Fig. 6B. SP-A in this region looks like a long, and thin ring chain. Black arrows in Fig. 6C point out regions of DWNTs that are covered and not covered by SP-A. The

inset in the right bottom corner of this figure shows a head of SP-A bound to DWNTs as pointed out by the black arrow.

The region that is not covered by a “monolayer” of well-organised SP-A heads looks thinner than the one that is covered. A possible explanation of this phenomenon will be discussed below. In addition, it must be said that the well-organised arrangement of the SP-A heads along the edge of DWNTs was a phenomenon found in all the TEM samples and in several independent experiments.

The binding of SP-D to carbon nanotubes also occurs through their heads. In Fig. 6E is shown the binding of two SP-D multimers (one at the top right and the other one at the bottom left) to a single DWNT. It is clear from this picture that several heads (at least three) of the SP-D multimer are bound to DWNTs. The SP-D heads

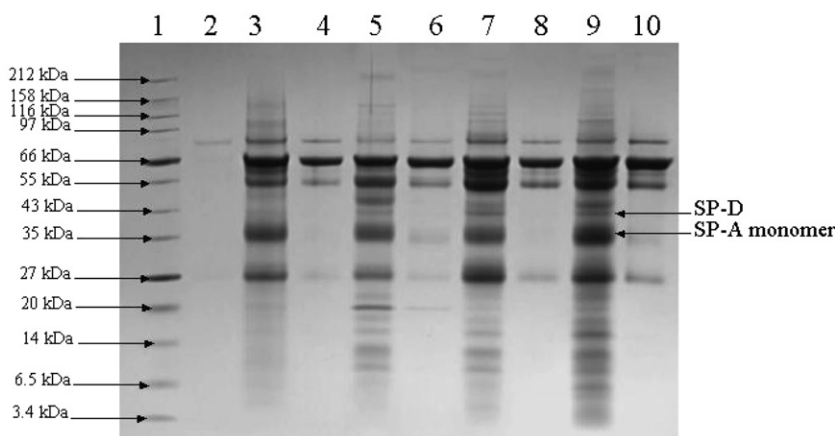


Fig. 7. Binding of the BALF supernatant protein SP-A and SP-D from four different patients to DWNT. Four different proteinosis patients randomly chosen were tested for the binding of SP-A and SP-D to DWNT. The protein concentration of each BALF supernatant sample was: Patient 1, 18 µg/ml, patient 2, 21 µg/ml, patient 3, 21 µg/ml, patient 4, 19 µg/ml. Protein concentration was measured by Bradford method as described in Section 2.3.2. Lane 1. Molecular weight markers; lane 2. Control experiment (BALF supernatant proteins bound to Sepharose); lane 3, 5, 7, 9. BALF supernatant proteins bound to DWNT-Sepharose; lane 4, 6, 8, 10. BALF supernatant (10 µl).

(8 nm diam) contact the DWNTs (1–3.5 nm diam) via a small portion of the total “head” surface area. As a result, only some heads (three) make contact with the DWNTs. The rest of the SP-D multimer heads hang from the DWNTs. However, this contact is enough to generate an interaction between SP-D and DWNT as shown in Fig. 3.

To verify reproducibility of SP-A and SP-D binding to DWNT in the presence of  $\text{Ca}^{2+}$  ions, we repeated the same experiment with three more different BALF supernatant samples originating from three different proteinosis patients. The same SP-A-concentrating effect was observed in all these samples (Fig. 7). In each case the SP-A bound to DWNTs (Fig. 7, tracks 3, 5, 7, 9) is greatly enriched in comparison to the SP-A concentration in the BALF supernatant samples (Fig. 7, tracks 4, 6, 8, 10). Additional protein bands appeared at high and low migration positions in the three different patients. These proteins were not examined further. In general the BALF protein pattern looked similar from each patient.

The amount of BALF supernatant SP-D and SP-A bound to DWNTs was estimated by Western blotting and SDS-PAGE, respectively as described in Section 2.3.9. It was found that the quantity of protein attached to 10 mg of DWNT was 0.86 µg for SP-D and 124 µg for SP-A (see Tables 2 and 3, respectively). Assuming that the quantity of SP-D in 20 L of BALF represents the con-

Table 2  
BALF supernatant SP-D bound to DWNT

	SP-D (µg)
BALF supernatant [50 ml] (109.62 ng/ml × 50 ml) <sup>a</sup>	5.48
BALF supernatant (5µl)	$5.4 \times 10^{-4}$
Sepharose–DWNT (5 µl) (25 µg DWNT)	$2.15 \times 10^{-3}$
Sepharose–DWNT column (10 mg DWNT in 1 ml)	0.86

<sup>a</sup> The concentration of SP-D in BALF was measured by ELISA as described in Section 2.3.8.

Table 3  
BALF supernatant SP-A bound to DWNT

	SP-A (µg)
BALF supernatant (50 ml)	2450
BALF supernatant (10 µl)	0.49
Sepharose–DWNT (10 µl) (50 µg of DWNT)	0.62
Sepharose–DWNT column (10 mg DWNT in 1 ml)	124

tent of 1 alveolar proteinosis lung, it would take about 12.5 g of non-aggregated DWNT to adsorb 50% of the SP-D in that one lung. Similar rationalisation indicates that 39.5 g of non-aggregated DWNTs will be needed to deplete SP-A 50% in the lung. For normal lungs, which have much lower levels of SP-A and SP-D than in alveolar proteinosis patients, the quantities of DWNT required for 50% depletion would be lower. There is not a precise estimation of the total quantity of SP-A, SP-D in surfactant from a whole normal lung.

By using 5 mg of DWNT and different volumes of BALF supernatant (12.5 ml, 25 ml and 50 ml), the same concentrating effect was observed. The amount of SP-A bound to DWNT slightly increases as the volume of BALF supernatant increases (Fig. 8). This indicates that 12.5 ml of BALF is enough to “saturate” the DWNT sites with SP-D and SP-A. However, as can be seen from the micrographs or by simple calculation there is not enough SP-D or SP-A present in the sample to fully coat the nanotube surface. This led us to further investigate the binding mechanisms between the surfactant proteins A and D and carbon nanotubes as well as to establish the probable binding sites. As mentioned before, the binding between carbon nanotubes and SP-A and SP-D is calcium-dependent. Crystallographic studies [13,14] have shown that  $\text{Ca}^{2+}$  ions mediate the normal reaction of binding of lectin domains to high-mannose sugars. The  $\text{Ca}^{2+}$  ions are coordinated by available carboxyl, carbonyl or amide moieties

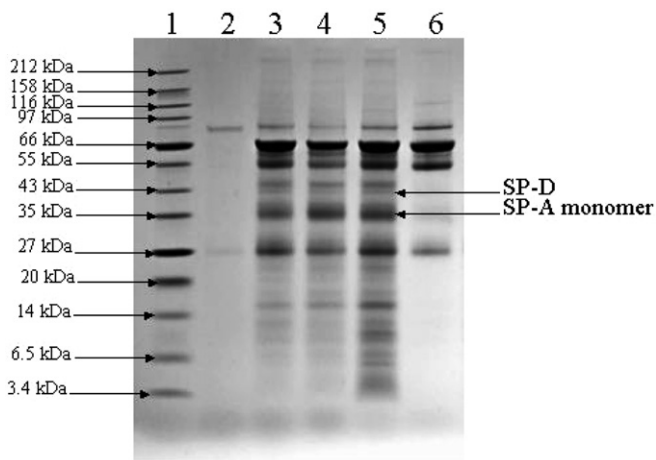


Fig. 8. BALF supernatant SP-A and SP-D bound to DWNT. DWNT suspended in Sepharose was used as an affinity medium to select SP-A and SP-D. Different volumes of undiluted BALF supernatant (12.5, 25 and 50 ml) previously dialysed in 10 mM HEPES, 140 mM NaCl, 0.15 mM CaCl<sub>2</sub>, pH 7.0 were loaded onto 1 ml Sepharose column containing 5 mg of DWNT. After removing unbound proteins by exhaustive washes with the dialysis buffer a suspension of the Sepharose–DWNTs mixture was analysed for the bound SP-A and SP-D by SDS-PAGE. Lane 1. Molecular weight marker, 2. Control experiment (BALF supernatant proteins bound to Sepharose); 3, 4, 5. SP-A and SP-D bound to DWNTs when passing 12.5, 25, and 50 ml of BALF supernatant through Sepharose–DWNT system. Lane 6. BALF supernatant (10 µl).

in the protein, and hydroxyl groups of the sugars. We therefore believe that SP-A and SP-D attach not directly to DWNT walls but to functional groups present on them. To verify this hypothesis we repeated the experiments using several batches of DWNT synthesised by the same procedure and exactly in the same conditions. We found that some batches proved better than others at binding with SP-A and SP-D. Thus, we conducted Infrared spectroscopy (IR) studies on two different batches: one that bound SP-A and SP-D, and another one that did not bind SP-A and

SP-D. IR confirmed the absence of detectable functional groups in the batch that did not bind SP-A or SP-D (Fig. 9a). Fig. 9b shows the IR spectrum that corresponds to a batch that did bind SP-A and SP-D. Seven peaks appear between 1500 and 3500 cm<sup>-1</sup> wave number. The bands at 1625 cm<sup>-1</sup> and 1721 cm<sup>-1</sup> are the most prominent. The absorbance at 1625 cm<sup>-1</sup> is characteristic of carbon-oxygen containing species and assigned to various forms of C–O, and C=C stretching. The peak at 1721 cm<sup>-1</sup> is characteristic of carbonyl compounds such as ketones, aldehydes, ester, and carboxylic acid groups. A peak at 2050 cm<sup>-1</sup> was not identified.

#### 4. Discussion

Binding of human plasma proteins including C1q, fibrinogen and high density lipoproteins to carbon nanotubes has been characterised by SDS-PAGE, mass spectrometry and N-terminal sequence analysis [1]. These binding reactions do not require divalent metal ions. In contrast the selective binding of BALF supernatant SP-A and SP-D to carbon nanotubes is Ca<sup>2+</sup>-ion dependent. The binding of SP-A and SP-D to carbon nanotubes can be stopped by using Ca<sup>2+</sup>-ion chelators such as EDTA (Fig. 3, track 3).

Three-dimensional crystallographic studies of the carbohydrate recognition domain (CRD) of SP-D and SP-A have reported the presence of one primary Ca<sup>2+</sup> ion in each CRD of both SP-D [13] and SP-A [14]. In SP-D there are three more Ca<sup>2+</sup> ions per CRD. In recombinant SP-D, the primary calcium ion (Ca1) is coordinated by the side chains of Glu<sup>321</sup>, Asn<sup>323</sup>, Glu<sup>329</sup>, Asn<sup>341</sup>, and Asp<sup>342</sup> residues [13]. The presence of carboxylic, aldehyde and ketone groups on the DWNT (Fig. 9b) is likely to provide coordination sites for the Ca<sup>2+</sup> ions bound to SP-A or SP-D. We found that some batches of pristine DWNT were unable to

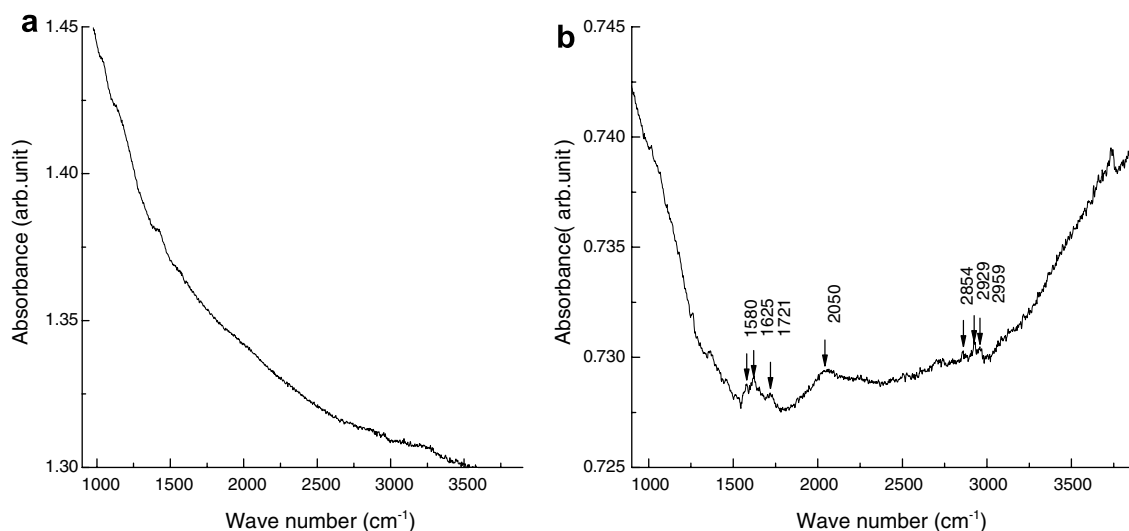


Fig. 9. IR spectra of “as-made” DWNTs before testing in protein binding experiments. (a) DWNTs which did not subsequently bind SP-A and SP-D, (b) DWNTs which did bind SP-A and SP-D.

fix SP-A and SP-D selectively from BALF. The difference in binding properties between batches correlated with the presence of functional groups (carboxylic, aldehyde or ketone) associated with the carbon nanotubes. These functional groups are likely to arise from “accidental” modification during synthesis and subsequent handling. Deliberate functionalisation of carbon nanotubes that involves the functional groups mentioned above will also influence the binding of SP-A and SP-D.

It has previously been shown in *in vivo* and *in vitro* experiments that carbon nanotubes produce an inflammatory reaction [3,15–17]. Recently, Muller et al. [3] reported that when multi-wall carbon nanotubes (6  $\mu\text{m}$  in length) and ground carbon nanotubes (0.7  $\mu\text{m}$  in length) reach the lungs, they are not rapidly eliminated. It was observed that carbon nanotubes remained in the lungs of mice over a period of at least two months. After this period, Muller et al. [3] measured in mouse BALF the levels of Tumor Necrosis Factor (TNF- $\alpha$ ) (a key mediator in inflammation and fibrosis) generated by the presence of different particles including asbestos (ASB) (Rhodesian Chrysotile “A”), ultrafine carbon black (CB) (ENSACO 250) carbon nanotubes (CNT) and ground carbon nanotubes (ground CNTs). *In vivo* experiments found production of TNF- $\alpha$  in response to both CNT and ground CNT. In general, these results suggest that carbon nanotubes are potentially toxic.

Lungs are the major sites of SP-A and SP-D production. These surfactant proteins constitute a major immune defense in the normal lung. They play an important role in limiting pulmonary infection, lung allergy and inflammation [18]. SP-A and SP-D perform their pulmonary function by enhancing the phagocytosis of invader organisms such as bacteria and virus [19]. The role of SP-A and SP-D in lung inflammation has two aspects. On the one hand they can generate a mild inflammatory response that may be crucial in preventing serious infections. On the other hand, they can promote chronic inflammation that may ultimately damage the lung. Similarly, the fact that SP-A and SP-D attach to DWNT can be considered as a double-edged sword. From one side, the binding of SP-A or SP-D to short nanotubes (less than a micron in length) could facilitate the phagocytosis process. Other particles such as asbestos which has similar morphology and that can have similar length to short carbon nanotubes ( $\sim 2 \mu\text{m}$ ) can be phagocytosed by alveolar macrophages [20]. Longer asbestos fibers which are too big to be taken up by one macrophage may become encapsulated by multiple macrophages, resulting eventually in formation of a granuloma. A similar fate could be expected for long nanotubes. Formation of multiple granulomas may reduce lung elasticity and gas exchange function. Granuloma formation after administration of CNTs has been reported [3,17]. In the short term, binding of SP-A and SP-D to potentially non-phagocytosable CNTs will sequester SP-A and SP-D, diminishing their concentration in the lung below normal levels. The binding capacity of DWNTs for SP-A and SP-D is low (Tables 2 and 3). Regardless of

the low capacity of DWNTs to sequester SP-A and SP-D there is a health risk to consider. Sequestration of a small amount of SP-A and SP-D by carbon nanotubes may produce a significant effect on susceptibility to infections.

The consequences of lowered SP-A and SP-D levels can be judged from the phenotypes of SP-A or SP-D knock-out mice: SP-D knock-out mouse studies have reported a decrease in resistance to some infections and emphysema-like alterations to the lungs [21,22]. These changes included a progressive accumulation of surfactant phospholipid in the lung tissue and alveolar space of the null mice and accumulation of apoptotic alveolar macrophages [23].

SP-A knock-out mice are less effective in clearing lung pathogens and therefore these mice are more susceptible to lung infection [24–26] by, for example Group B streptococci (GBS). GBS are common pathogens in premature and term neonates. Clearance of GBS from the lungs of SP-A (–/–) mice was significantly reduced compared to normal mice. Furthermore, it was observed that GBS proliferated in the lungs of SP-A (–/–) mice and was detectable in the spleen at 24 and 48 h [24]. SP-A-deficient animals also present decreased phagocytosis and oxidant metabolism in response to instilled GBS. These findings support the idea that SP-A plays an important role in innate immunity by protecting the lung from microbial infection and injury. The SP-D and SP-A knock-out mice are relevant for our study in the sense that they can help us to hypothesise the toxicological effects that could arise from the sequestration of SP-A and SP-D by carbon nanotubes [27,28]. Although sequestration of SP-A, SP-D by carbon nanotubes is not equivalent to a complete absence of the proteins, the sequestration would limit the diffusion mobility of the proteins and would lower the effective concentrations in the lungs. A small number of publications indicate disease correlation with lowered levels of SP-A in humans. These include association of lowered SP-A levels with asthma and allergen-induced bronchial inflammation [4,29].

Although there are many discrepancies in the results reported on the effects produced by carbon nanotubes in the lungs of animals such as rats, mice and hamsters, it is worthwhile to be aware of the potential health risks of these nanomaterials. Muller et al. [30] have reviewed the most recent findings reported so far in the area of pulmonary toxicity of carbon nanotubes. In this review it is shown that there are contrary opinions on the toxicity of carbon nanotubes. For example, some scientists interpret their results to conclude that carbon nanotubes are unlikely to be associated with health risk [31]. In contrast, the interpretation of Muller et al. [3] and others [15–17] is that carbon nanotubes have potential to stimulate fibrosis and emphysema. Currently, it is important to point out that regardless of the inaccuracy of the methodology used to investigate the pulmonary toxicity of carbon nanotubes, the major conclusion is that carbon nanotubes are toxic to some extent. This is based not only in the trend that can be observed in all the most recent papers in this area but also on the analogies that exists in the toxicity (size and

morphology) with other well-characterised toxic materials such as asbestos and carbon black.

Taking into account the considerations mentioned above, there are several facts that lead us to think that the inflammatory response induced by carbon nanotubes *in vitro* and *in vivo* experiments may be correlated to the SP-A and SP-D functions. These are: the formation of bronchiolar granulomas around focal aggregate of CNTs, the capacity of carbon nanotubes to stimulate lung cells to produce TNF- $\alpha$ , and the accumulation of collagen in the lungs of animals treated with carbon nanotubes and ground carbon nanotubes. The granuloma formation reported by Muller and co workers [3] was similar to that reported previously in the airways of rats by Warheit et al. [2]. Lam et al. [15] also reported the presence of those granulomas in mouse interstitium. This is consistent with a recent study in human lung emphysema describing a thickening of the interstitium in the remaining alveolar walls because of the increase in both elastin and collagen. The alveolar septa in these areas were thickened, and lamellar bodies in type II cells were prominent compared with-type mice. Previously it was mentioned that formation of granuloma may reduce lung elasticity and gas exchange. In addition, it is likely that changes in the lamellar bodies in type II cells alter the presence of SP-A.

## 5. Conclusion

In conclusion, this study contributes to the elucidation of a molecular mechanism involved in pulmonary toxicity of carbon nanotubes. In addition, this communication opens up new routes of research in this area, aimed at obtaining a better understanding of the role of the sequestration of SP-A and SP-D by carbon nanotubes. It also suggests that functionalisation while lowering the toxicity in some nanomaterials might also have toxicity implications of its own [32]. More studies are needed to investigate if surface modification such as the one done in doped nitrogen multi-walled carbon nanotubes (CN<sub>x</sub>) can be less susceptible to attract impurities and therefore to prevent the sequestration of SP-A and SPD. Thus, they could be less toxic for the lungs as reported recently by Carrero-Sanchez et al. [33].

## Acknowledgments

This work was supported partly by the Medical Research Council, UK. C. Salvador-Morales acknowledges the Mexican National Council for Science and Technology (CONACYT) for a Graduate scholarship. We thank Mr. A.C. Willis for the N-terminal sequence analysis measurements and Miss Roona Deb for providing the SP-A protein.

## References

[1] Salvador-Morales C, Flahaut E, Sim E, Sloan J, Green MLH, Sim RB. Complement activation and protein adsorption by carbon nanotubes. *Mol Immunol* 2006;43(3):193–201.

[2] Warheit DB, Laurence BR, Reed KL, Roach DH, Reynolds GAM, Webb TR. Comparative pulmonary toxicity assessment of single-wall carbon nanotubes in rats. *Toxicol Sci* 2004;77(1):117–25.

[3] Muller J, Huaux F, Moreau N, Misson P, Heilier JF, Delos M, et al. Respiratory toxicity of multi-wall carbon nanotubes. *Toxicol Appl Pharmacol* 2005;207(3):221–31.

[4] Hickling TP, Clark H, Malhotra R, Sim RB. Collectins and their role in lung immunity. *J Leukoc Biol* 2004;75(1):27–33.

[5] Flahaut E, Bacsá R, Peigney A, Laurent C. Gram-scale CCVD synthesis of double-walled carbon nanotubes. *Chem Commun* 2003;12:1442–3.

[6] Kim JU, Furtado CA, Liu X, Chen G, Eklund PC. Raman and IR spectroscopy of chemically processed single-walled carbon nanotubes. *J Am Chem Soc* 2005;127(44):15437–45.

[7] Murray E, Khamri W, Walker MM, Eggleton P, Moran AP, Ferris JA, et al. Expression of surfactant protein D in the human gastric mucosa and during helicobacter pylori infection. *Infect Immun* 2002;70(3):1481–7.

[8] Palaniyar N, Nadesalingam J, Clark H, Shih MJ, Dodds AW, Reid KB. Nucleic acid is a novel ligand for innate, immune pattern recognition collectins surfactant proteins A and D and mannose-binding lectin. *J Biol Chem* 2004;279(31):32728–36.

[9] Bradford MM. A rapid and sensitive method for the quantitation of microgram quantities of protein utilizing in the principle of protein-dye binding. *Anal Biochem* 1976;72(1–2):248–54.

[10] Suwabe A, Masson RJ, Voelker DR. Calcium dependent association of surfactant protein A with pulmonary surfactant: application to simple surfactant protein A purification. *Arch Biochem Biophys* 1996;327(2):285–91.

[11] Strong P, Kishore U, Morgan C, Lopez Bernal A, Singh M, Reid KB. A novel method of purifying lung surfactant proteins A and D from the lung lavage of alveolar proteinosis patients and from pooled amniotic fluid. *J Immunol Methods* 1998;220(1–2):139–49.

[12] Hoppe HJ, Reid KB. Trimeric C-type lectin domain in host defence. *Structure* 1994;2:1129–33.

[13] Hakansson K, Lim NK, Hoppe HJ, Reid KBM. Crystal structure of the trimeric  $\alpha$ -helical coiled-coil and the three lectin domains of human lung surfactant protein D. *Structure* 1999;7(3):255–64.

[14] Head JF, Mealy TR, McCormack FX, Seaton BA. Crystal structure of trimeric carbohydrate recognition and neck domains of surfactant protein A. *J Biol Chem* 2003;278(44):43254–60.

[15] Lam CW, James JT, McCluskey R, Hunter RL. Pulmonary toxicity of single-wall carbon nanotubes in Mice 7 and 90 days after intratracheal instillation. *Toxicol Sci* 2004;77(1):126–34.

[16] Murr LE, Garza KM, Soto KF, Carrasco A, Powell TG, Ramirez DA, et al. Cytotoxicity assessment of some carbon nanotubes and related carbon nanoparticle aggregates and the implications for anthropogenic carbon nanotube aggregates in the environment. *Int J Environ Res Public Health* 2005;2(1):31–42.

[17] Shvedova AA, Castranova V, Kisin ER, Murray AR, Schwegler-Berry D, Gandelsman VZ, et al. Exposure to nanotube material: assessment of nanotube cytotoxicity using human keratinocyte cells. *J Toxicol Environ Health* 2003;66(20):1909–26.

[18] Kishore U, Lopez Bernal A, Kamran MF, Saxena S, Singh M, Sarma PU, et al. Surfactant proteins SP-A and SP-D in human health and disease. *Arch Immunol Ther Exp* 2005;53:317–99.

[19] Hartshorn KL, Crouch E, White MR, Colamussi ML, Kakkanatt A. Pulmonary surfactant proteins A and D enhance neutrophil uptake of bacteria. *Am J Physiol* 1998;274(6):L958–69.

[20] Skinner HCW, Ross M, Frondel C. Asbestos and other fibrous materials. Oxford: Oxford University Press; 1988. pp. 103–239.

[21] Botas C, Poulain F, Akiyama J, Brown C, Allen L, Goerke J, et al. Altered surfactant homeostasis and alveolar type II cell morphology in mice lacking Surfactant protein D. *Proc Natl Acad Sci USA* 1998;95(20):11869–74.

[22] Korfhagen TR, Sheftelyevich V, Burhans MS, Bruno MD, Ross GF, Wert SE, et al. Surfactant protein-D regulates surfactant phospholipid homeostasis in vivo. *J Biol Chem* 1998;273(43):28438–43.

- [23] Wert SE, Yoshida M, LeVine AM, Ikegami M, Jones T, Ross GF, et al. Increased Metalloproteinase activity, oxidant production, and emphysema in surfactant protein D gene-inactivated mice. *Proc Natl Acad Sci* 2000;97(11):5972–7.
- [24] Korfhagen TR, LeVine AM, Whitsett JA. Surfactant protein A (SP-A) gene targeted mice. *Biochim Biophys Acta* 1998;1408(2–3): 296–302.
- [25] Korfhagen TR, Bruno MD, Ross GF, Huelsman KM, Ikegami M, Jobe AH, et al. Altered surfactant function and structure in SP-A gene targeted mice. *Proc Natl Acad Sci USA* 1996;93(18): 9594–9.
- [26] Atochina EN, Beck JM, Preston AM, Haczku A, Tomer Y, Scanlon ST, et al. Enhanced lung injury and delayed clearance of pneumocystis carinii in surfactant protein-A deficient mice: attenuation of cytokine response and reactive oxygen–nitrogen species. *Infect Immun* 2004;72(10):6002–11.
- [27] Hawgood S, Ochs M, Jung A, Akiyama J, Allen L, Brown C, et al. Sequential targeted deficiency of SP-A and -D leads to progressive alveolar lipoproteinosis and emphysema. *Am J Physiol Lung Cell Mol Physiol* 2002;283(5):L1002–10.
- [28] Madan T, Reid KB, Singh M, Sarma PU, Kishore U. Susceptibility of mice genetically deficient in the surfactant protein (SP)-A or SP-D gene to pulmonary hypersensitivity induced by antigens and allergens of *Aspergillus fumigatus*. *J Immunol* 2005;174(11):6943–54.
- [29] Hohlfeld JM. The role of surfactant in asthma. *Respir Res* 2002;3(4):1–8.
- [30] Muller J, Huaux F, Lison D. Respiratory toxicity of carbon nanotubes: how worried should we be? *Carbon* 2006;44(6):1048–56.
- [31] Huczko A, Lange H, Calko E, Grubek-Jaworska H, Droszcz P. Physiological testing of carbon nanotubes: are they asbestos-like? *Fullerene Sci Technol* 2001;9(2):251–4.
- [32] Colvin V. Non-toxic materials: the role of surface chemistry. Abstracts of papers, 231st ACS National Meeting. American Chemical Society, 2006.
- [33] Carrero-Sanchez JC, Elias AL, Mancilla R, Arrellin G, Terrones H, Laclette JP, et al. Biocompatibility and toxicological studies of carbon nanotubes doped with nitrogen. *Nano Lett* 2006;6(8):1609–16.
- [34] Murray E. Roles of lung surfactant proteins SP-A and SP-D in innate immunity and allergy. Oxford UK, University of Oxford, D. Phil. thesis, 2001.